Invited Paper

Electrical characterization of $Al_xGa_{1-x}N$ for UV photodetector applications

A. Saxler*[a], M. Ahoujja[a], W. C. Mitchel[a], P. Kung[b], D. Walker[b], M. Razeghi[b]

[a]Air Force Research Laboratory, Materials and Manufacturing Directorate, Sensor Materials Branch, Wright-Patterson AFB, OH 45433-7707

[b]Center for Quantum Devices, Department of Electrical and Computer Engineering, Northwestern University, Evanston, IL 60208

ABSTRACT

Ultraviolet photodetectors have many military and commercial applications. However, for many of these applications, the photodetectors must be solar blind. This means that the photodetectors must have a cutoff wavelength of less than about 270 nm. Semiconductor based devices would then need energy gaps of over 4.6 eV. In the $Al_xGa_{1-x}N$ system, the aluminum mole fraction, x, required is over 40%. As the energy gap is increased, doping becomes much more difficult, especially p-type doping. This report is a study of the electrical properties of $Al_xGa_{1-x}N$ to enable better control of the doping. Magnesium doped p-type $Al_xGa_{1-x}N$ has been studied using high-temperature Hall effect measurements. The acceptor ionization energy has been found to increase substantially with the aluminum content. Short-period superlattices consisting of alternating layers of GaN:Mg and AlGaN:Mg were also grown by low-pressure organometallic vapor phase epitaxy. The electrical properties of these superlattices were measured as a function of temperature and compared to conventional AlGaN:Mg layers. It is shown that the optical absorption edge can be shifted to shorter wavelengths while lowering the acceptor ionization energy by using short-period superlattice structures instead of bulk-like AlGaN:Mg. Silicon doped n-type films have also been studied.

Keywords: GaN, gallium nitride, AlGaN, aluminum gallium nitride, Hall effect, ultraviolet photodetectors, short-period superlattice, p-type doping, magnesium doping

1. INTRODUCTION

The aluminum gallium nitride (AlGaN) material system has an energy gap ranging from 3.4 to 6.2 eV while the lattice constant only varies by 2.5%. This makes it highly desirable for many device applications. For instance, this is currently the most promising semiconductor system for truly solar blind photodetectors[1] with cutoff wavelengths shorter than 270 nm. Many other applications exist for the III-Nitrides in high-power and high-temperature electronics,[2] and blue and ultraviolet light emitting and laser diodes,[3] but materials issues still dominate. A major problem is the doping - especially as the aluminum concentration is increased. Silicon is the preferred n-type dopant, and magnesium is the preferred p-type dopant. Both are substitutional for the gallium atom in GaN. Germanium is another n-type dopant that has been successfully used for AlGaN.[4] N-type doping of the III-Nitrides using selenium[5] and sulfur[6] has not been very successful because of the difficulty of incorporation onto the nitrogen sites. We have previously reported III-Nitride growth,[7-10] characterization,[11,12] and photodetectors.[13,14] This paper will treat the electrical properties and doping techniques for both n-type and p-type AlGaN.

The III-Nitride layers were grown in a horizontal low-pressure organometallic vapor phase epitaxy reactor manufactured by AIXTRON (AIX 200/4 HT). All of the thin films discussed in this paper were grown on (0001) sapphire substrates with a high temperature AlN nucleation layer. The precursors used were trimethylgallium (TMGa) or triethylgallium (TEGa) as the gallium source, trimethylaluminum (TMAl) for aluminum, ammonia (NH_3) for nitrogen, dilute silane (SiH_4) for silicon, and biscyclopentadienylmagnesium (Cp_2Mg) for magnesium.

* Correspondence: Email: saxleraw@ml.wpafb.af.mil; Telephone: 937 255 4474 x3273; Fax: 937 255 4913

Part of the SPIE Conference on Photodetectors: Materials and Devices IV
San Jose, California • January 1999
SPIE Vol. 3629 • 0277-786X/99/$10.00

2. N-TYPE AlGaN

GaN films are easily doped with silicon using silane diluted in hydrogen as a precursor. The carrier concentration increases linearly with the silane flow. It is interesting to note that the intercept is negative (Figure 1(a)), possibly indicating that there are a large number of l vels acting as deep acceptors in the undoped insulating GaN layers. As seen in Figure 1 (b), the room temperature Hall mobility also increases with higher doping in this regime, which is again consistent with compensation by deep acceptors. The x-ray rocking curve broadens somewhat as the doping increases as seen in Figure 2 showing that the structural properties are also affected by doping.

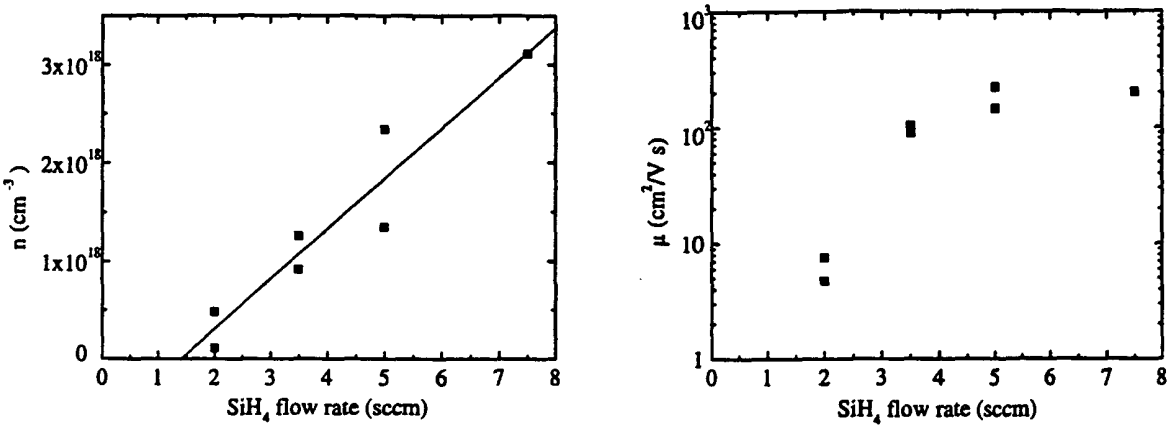

Figure 1. The room temperature carrier concentration of GaN increases linearly (a) and the mobility increases (b) with the dopant flow.

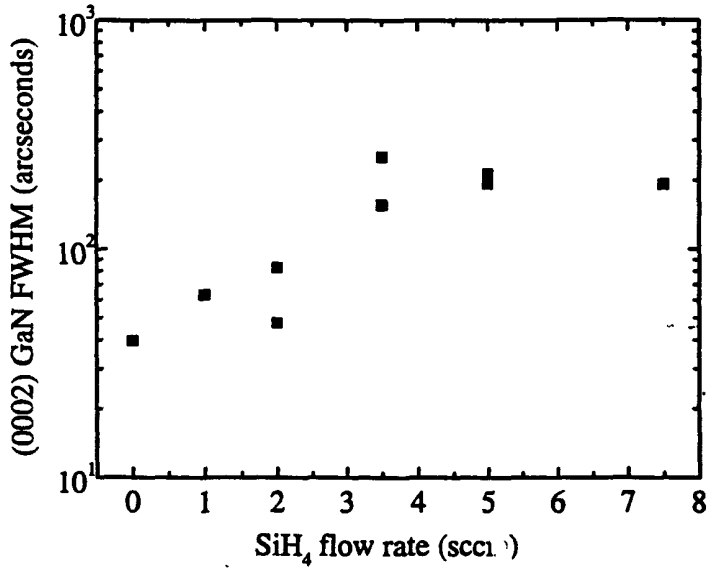

Figure 2. The X-ray rocking curve of GaN broadens somewhat with increased dopant flow.

AlGaN films with low aluminum content also exhibit linear increases in the carrier concentration with increases in the SiH_4 flow rate as shown in Figure 3. The undoped films were insulating, again indicating the possibility of compensation by a

deep acceptor level. From the intercept of the line, a net acceptor concentration $N_a - N_d$ of about 7 x 10^{17} cm^{-3} can be estimated for these undoped $Al_{0.2}Ga_{0.8}N$ films.

Figure 4 shows the temperature dependent Hall effect data for these samples. The apparent electron concentration is nearly temperature independent, but the minima in the curves are indicative of a second conduction path such as an impurity band or interfacial layer. The changes in the resistivity with temperature largely track the mobility, because of the relatively flat carrier concentration curve. The increasing mobility to high temperatures is consistent with scattering by ionized impurities such as deep acceptors.

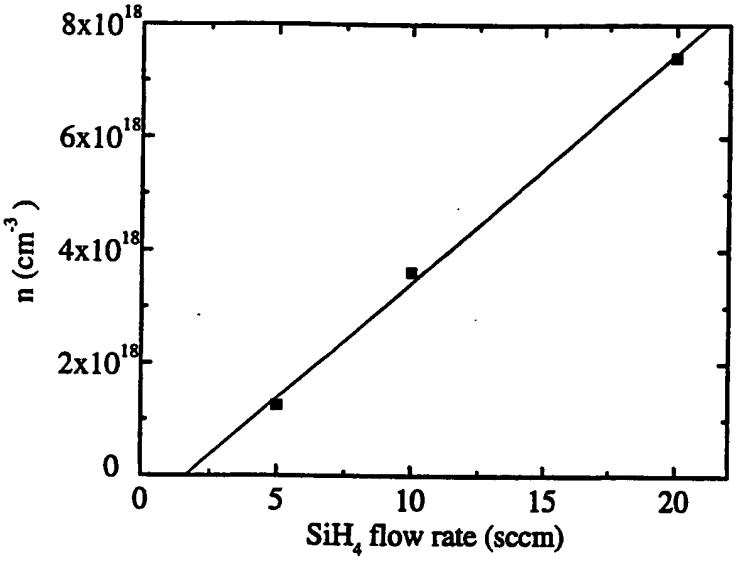

Figure 3. The room temperature electron concentration is a linear function of the dilute SiH4 flow rate for $Al_xGa_{1-x}N$ with x = 0.2.

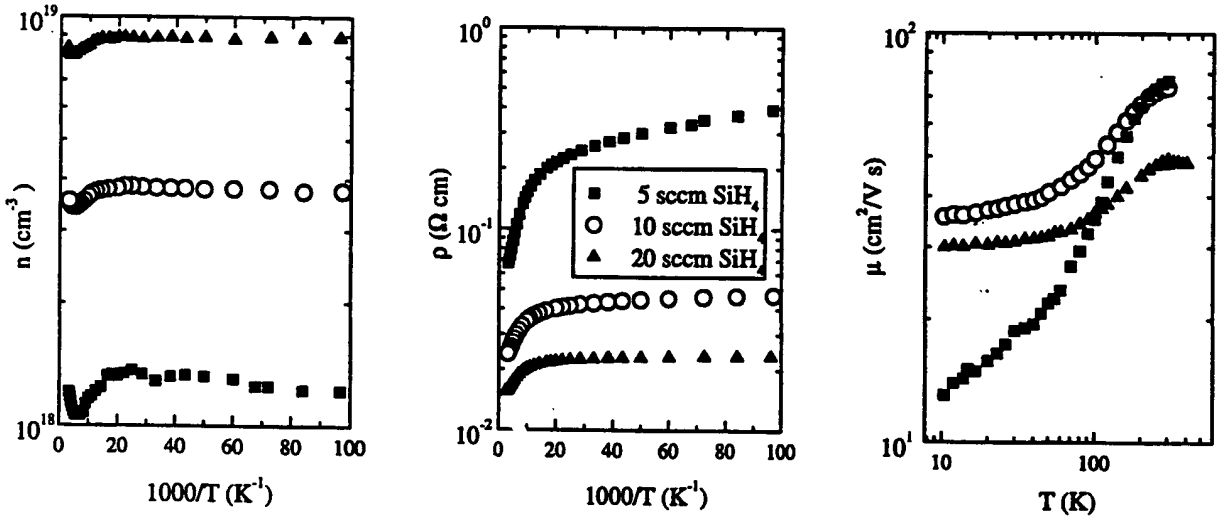

Figure 4. Electrical data for AlGaN (x=0.2) with different silane flow rates.

The silicon doping of $Al_xGa_{1-x}N$ films has also been studied as a function of the aluminum composition x. Assuming Vegard's law applies and the films are relaxed, the composition was determined by measuring the *c* lattice constant. As x increases, the films become progressively more difficult to dope. As seen in Figure 5, the resistivity increases by several orders of magnitude as x is increased to over 50% while the dopant flow remained constant.

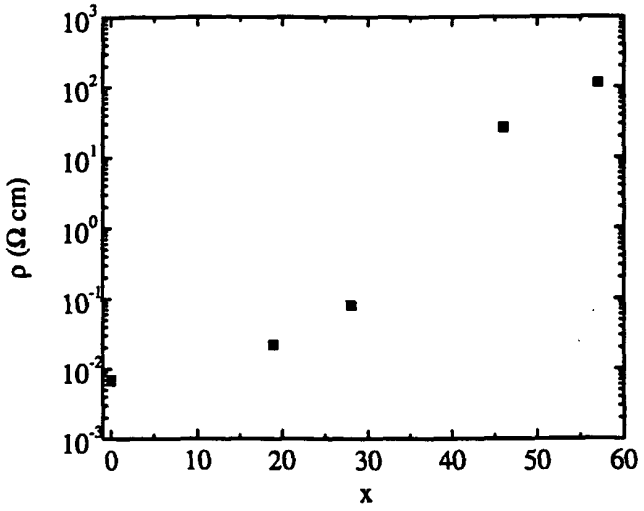

Figure 5. The room temperature resistivity is plotted as a function of x in $Al_xGa_{1-x}N$ doped with 10 sccm of dilute SiH_4.

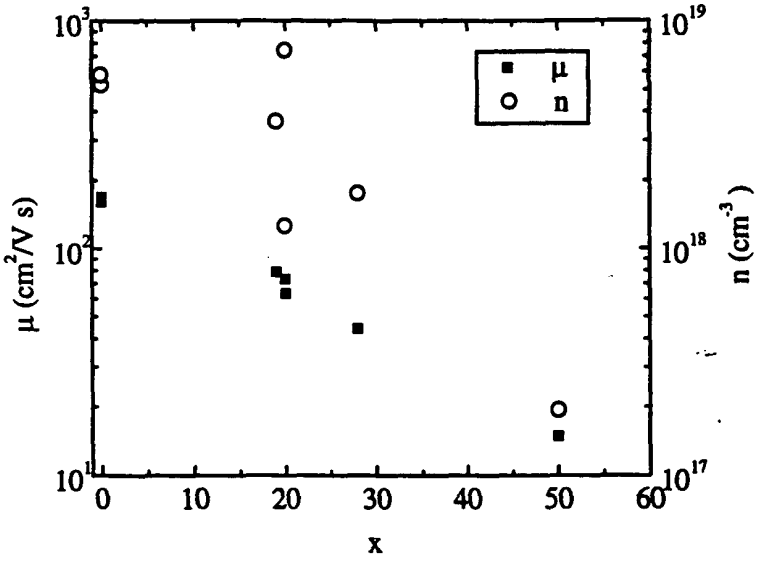

Figure 6. The room temperature mobility and carrier concentration as a function of x.

As can be seen in Figure 6, this is primarily due to a decrease in the carrier concentration, although the mobility also decreases significantly. The lower carrier concentration at higher aluminum concentrations could be due to higher compensation, a higher ionization energy, or lower incorporation efficiency of the silicon dopant. The mobility may

decrease because of an increased effective mass, alloy scattering, or larger concentrations of defects and impurities. The lower carrier concentrations may also lead to poorer screening of charged scatterers.

The temperature dependent resistivity was also measured for various aluminum concentrations with the same silane flow rates. The activation energy was very low up to aluminum concentrations f 50%. For an aluminum concentration of 70%, however, the activation energy of the resistivity jumped to 0.68 eV. Instead of a sudden increase in the silicon ionization energy, it is possible that this deep level is related to a cation vacancy or a oxygen DX center.[15] The carrier type of this high resistivity sample was not determined because of the very low mobility.

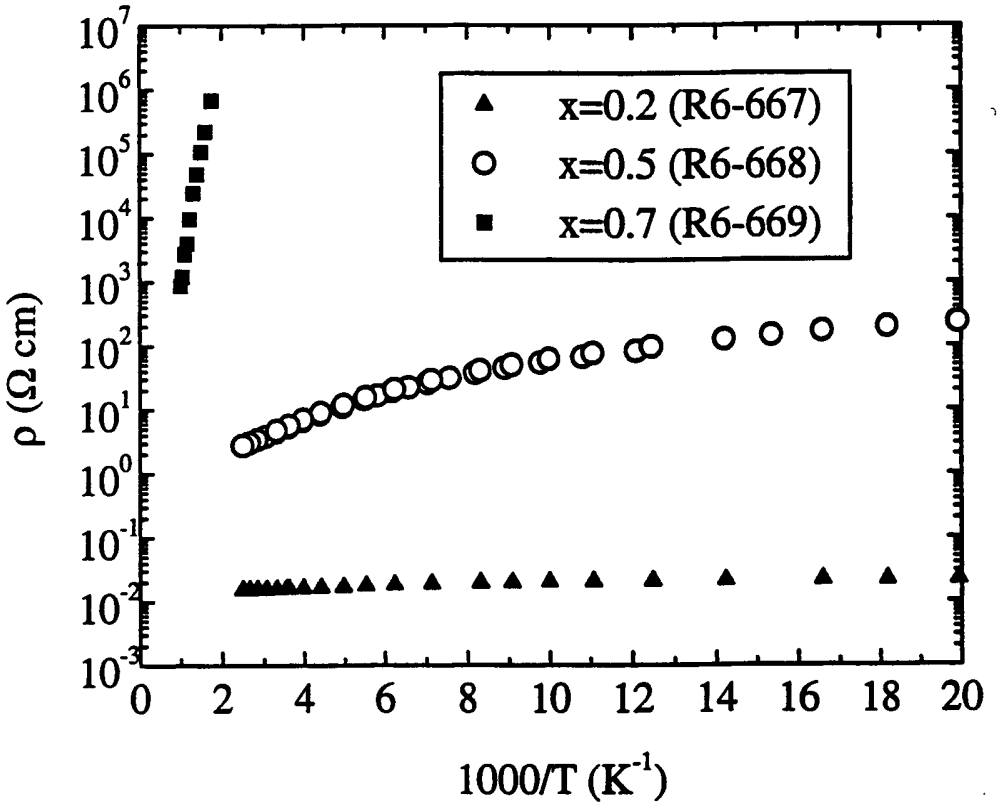

Figure 7. Resistivity as a function of reciprocal temperature for identically silicon doped AlGaN with different aluminum mole fractions.

3. P-TYPE AlGaN

3.1. Bulk-like AlGaN:Mg

One of the most important remaining issues is the p-type doping of the III-Nitrides, especially AlGaN with high aluminum mole fractions because of the relatively deep acceptors.[15-19] The p-type doping of GaN is a critical step for the fabrication of bipolar III-Nitride devices including LED's, laser diodes, and p-i-n photodetectors. Unfortunately, this is not an easy task. As we will see, two major problems exist for the doping. The first problem is the large ionization energy of the dopants, which results in a much lower free hole carrier concentration than the dopant concentration. The second challenge is the low solubility of the dopant in the material. The resistivity of the material is the best metric for comparing p-type films. This is due to the low mobility of p-type AlGaN which results in a low Hall voltage and a poor signal to noise ratio for the carrier concentration and mobility.

From Figure 8(a), it is apparent that the carrier concentration is extremely sensitive to the dopant flow rate. The resistivity varies over several orders of magnitude for variation in the flow rate of only about a factor of ten. There is a narrow relative minimum in the resistivity for which the p-type doping is successful. The initial steep decline in the resistivity may be due to factors such as reduced compensation of acceptors by donors. The onset of the increase in resistivity may be due to the formation of magnesium nitride or other phases that disrupt the quasi-two dimensional growth of GaN. In any case, the structural properties of the GaN are adversely affected by heavy doping with Cp_2Mg. As seen in Figure 8(b), the x-ray linewidth increases as the doping increases, indicating the deterioration of the structural perfection. The surface morphology also became rougher as observed by SEM for heavily doped films.

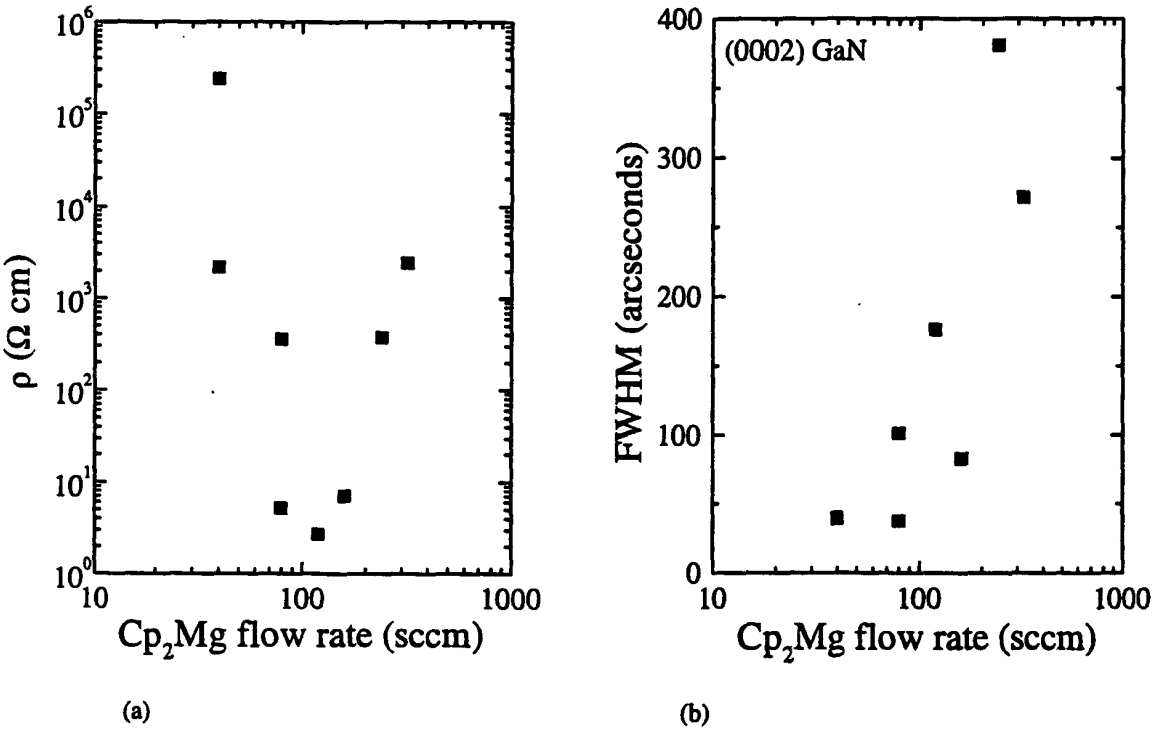

Figure 8. (a) Resistivity at room temperature as a function of the magnesium flow rate indicates that the doping of GaN is extremely sensitive to the flow rate and is nonlinear. (b) The x-ray rocking curve linewidth increases as the magnesium doping is increased.

The carrier concentration is a very strong function of temperature, indicative of a large dopant ionization energy. The mobility is only weakly dependent on temperature, so the temperature dependent resistivity primarily reflects the carrier concentration variation with temperature.

The AlGaN:Mg layers have higher activation energies and higher resistivities than the GaN layers. As shown in Figure 9, the room temperature resistivity of a series of AlGaN:Mg layers increases logarithmically as the aluminum concentration is increased for the same magnesium dopant flow. In addition to the increase in the impurity ionization energy that is probably the dominant factor, additional factors may be responsible including reduced mobility or a lower magnesium incorporation rate. The mobility is probably reduced by an increased effective mass and increased scattering due to higher concentrations of defects and ionized impurities. The oxygen concentration is expected to increase with the aluminum concentration, compensating the p-type material and contributing ionized impurity scattering centers.

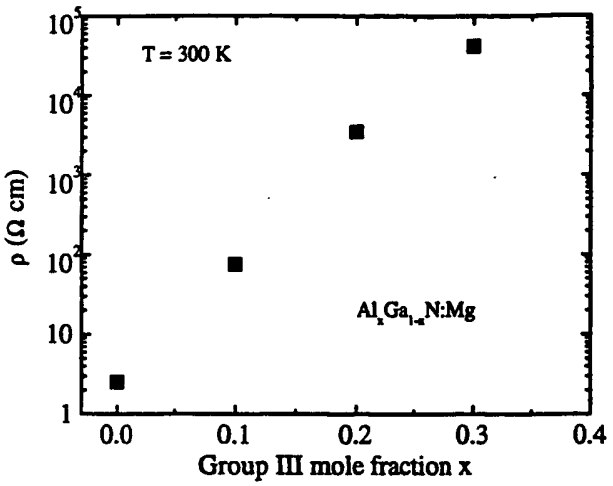

Figure 9. The room temperature resistivity of AlGaN increases by several orders of magnitude as the Al content is increased.

The activation energy of the resistivity as a function of the aluminum fraction for AlGaN:Mg samples is obtained by fitting the temperature dependent resistivities. This activation energy increases rapidly as the bandgap increases, as will be seen in the next section.

3.2 Magnesium doped short-period superlattices

In this section, we present the p-type doping of AlGaN short period superlattices (SPSL's) with the motivation of reducing acceptor ionization energies and compare this technique to the doping of single AlGaN layers. Also, superlattices of AlGaN have been used for reducing cracking in the confinement layers of III-Nitride lasers,[20] so it is useful to understand their electrical properties.

A 50 nm thick, high-temperature AlN nucleation layer was deposited prior to an AlGaN layer or superlattice at 1050°C with a total thickness of 0.7 μm. Following the growth, the samples were annealed in the reactor at 900°C in nitrogen for ten minutes to remove the hydrogen passivation of the acceptors. Table I shows the structures of the SPSL's including the layer thicknesses and aluminum concentrations. The cutoff wavelengths and acceptor ionization energies of the SPSL's studied are also shown in the table. (The arbitrarily chosen $\lambda_{50\%}$ is defined as the wavelength at which half of the light is transmitted through the film. This wavelength falls on the steep slope of the transmission curve and corresponds to about 10^4 cm^{-1} for these 0.7 μm thick samples.)

Table I. Sample data including superlattice layer thicknesses, composition of the $Al_xGa_{1-x}N$ layer, cutoff wavelengths, and acceptor ionization energies.

Sample	t_{GaN} (Å)	t_{AlGaN} (Å)	x	$\lambda_{50\%}$ (nm)	E_A (meV)
813	23	23	0.30	350	124
821	39	8	0.30	361	116
824	8	17	0.45	326	268
825	8	9	0.45	335	240

Figure 10 is a diagram of the valence band of a SPSL, drawn without any band bending. $E_{A,GaN}$ and $E_{A,AlGaN}$ are the acceptor ionization energies in GaN and AlGaN respectively. ΔE_{VB} is the valence band offset, and ΔE_{SL} is the offset of the bottom of the first miniband of the SPSL from the valence band of GaN. For true superlattice behavior, the barriers must be very thin so the wavefunction can penetrate in spite f the large effective hole mass. The positions of the minibands can

be simply calculated,[21] but the effective masses and valence band offsets are not yet well known for the AlGaN system. Using the diagram, the acceptor ionization energy is given by one of the following equations:

$$E_{A,SPSL} = E_{A,AlGaN} + \Delta E_{SL} - \Delta E_{VB} \quad (1)$$

$$E_{A,SPSL} = E_{A,GaN} + \Delta E_{SL} \quad (2)$$

If each constituent layer is p-type, the smaller of Eqs. (1) and (2) will be the initial ionization energy. However, if the AlGaN layer were fully compensated as is likely in very high aluminum content layers, Eq. (2) would be relevant.

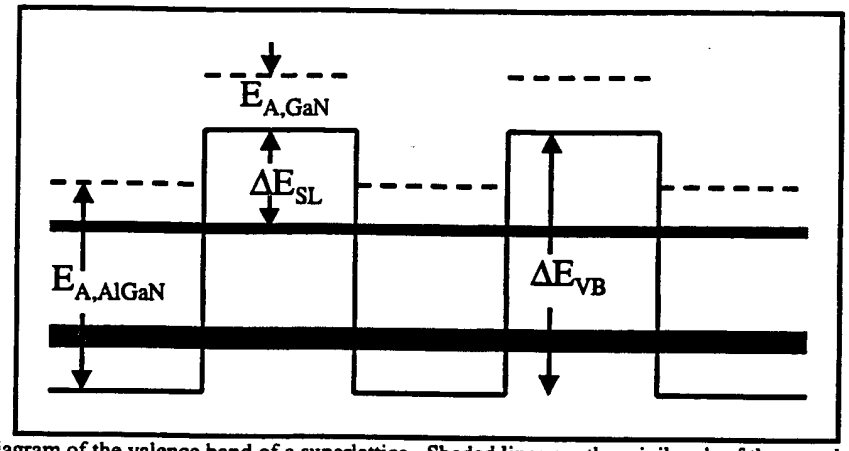

Figure 10. Schematic diagram of the valence band of a superlattice. Shaded lines are the minibands of the superlattice. Dashed lines are the dopant levels in their host material.

X-ray diffraction curves were obtained using a Philips HRD system with a monochromator utilizing four (220) Ge reflections. Figure 11 shows the ω/2θ curve of a Mg doped GaN/AlGaN SPSL. In addition to the main peak, both the AlN buffer layer peak and the -1 superlattice peak are visible. The superlattice period calculated from the peak positions agrees with the expected thickness based on the growth rates of the constituent layers of the SPSL.

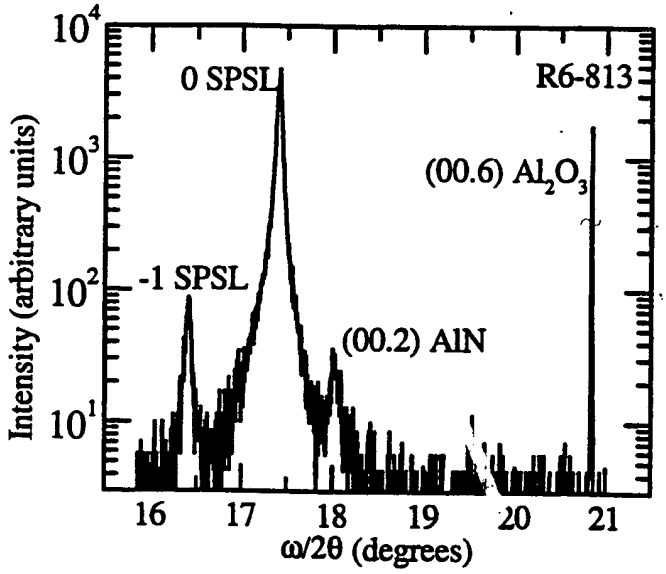

Figure 11. X-ray diffraction ω/2θ curve f a magnesium doped GaN/AlGaN SPSL.

UV-visible transmission curves were obtained using a dual beam spectrometer with a sapphire substrate in the reference beam. Figure 12 shows the optical transmission curve for a SPSL compared with curves for its constituent GaN:Mg and AlGaN:Mg layers. As expected, the onset of the absorption edge of the SPSL is clearly shifted to a shorter wavelength than GaN. Once the absorption edge is reached, the bulk-like binary and ternary films quickly absorb all of the incident light, within the limit of the background noise. This contrasts with the transmission curve of the SPSL, which has a small peak below the initial absorption edge. This is consistent with absorption between the allowed energy bands of the SPSL.

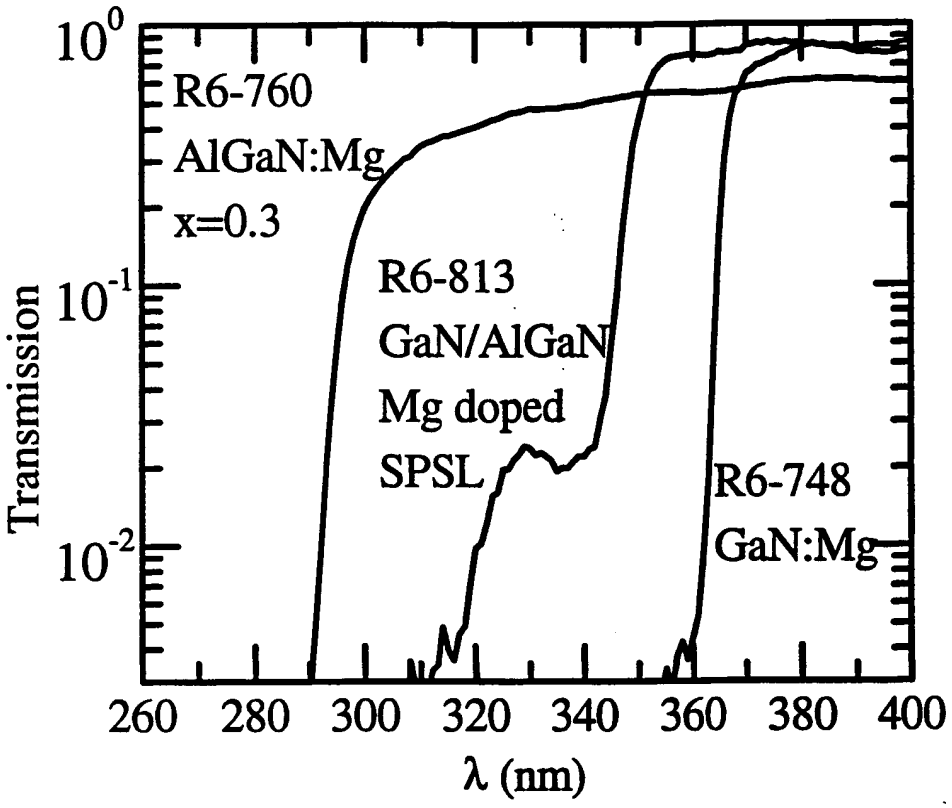

Figure 12. Optical transmission of III-Nitride films.

Figure 13 shows the resistivity as a function of temperature for a magnesium doped GaN/AlGaN SPSL and its constituent layers. Temperature dependent Hall effect and resistivity measurements were taken in the van der Pauw configuration in a nitrogen or helium atmosphere. The hole concentration could not always be obtained because the noise was often larger than the Hall voltage, largely because of the low hole mobilities that were typically less than 10 cm^2/V s. Assuming the mobility is comparatively temperature independent, the acceptor ionization was extracted by assuming resistivity is inversely proportional to $T^{3/2}e^{-E_A/kT}$ where T is the absolute temperature, E_A is the acceptor ionization energy, and k is the Boltzmann constant. Only the steepest part of the curve was used in the fit, to exclude hopping conduction at the lowest temperatures and both saturation and irreversible changes, which sometimes occurred at the highest temperatures.

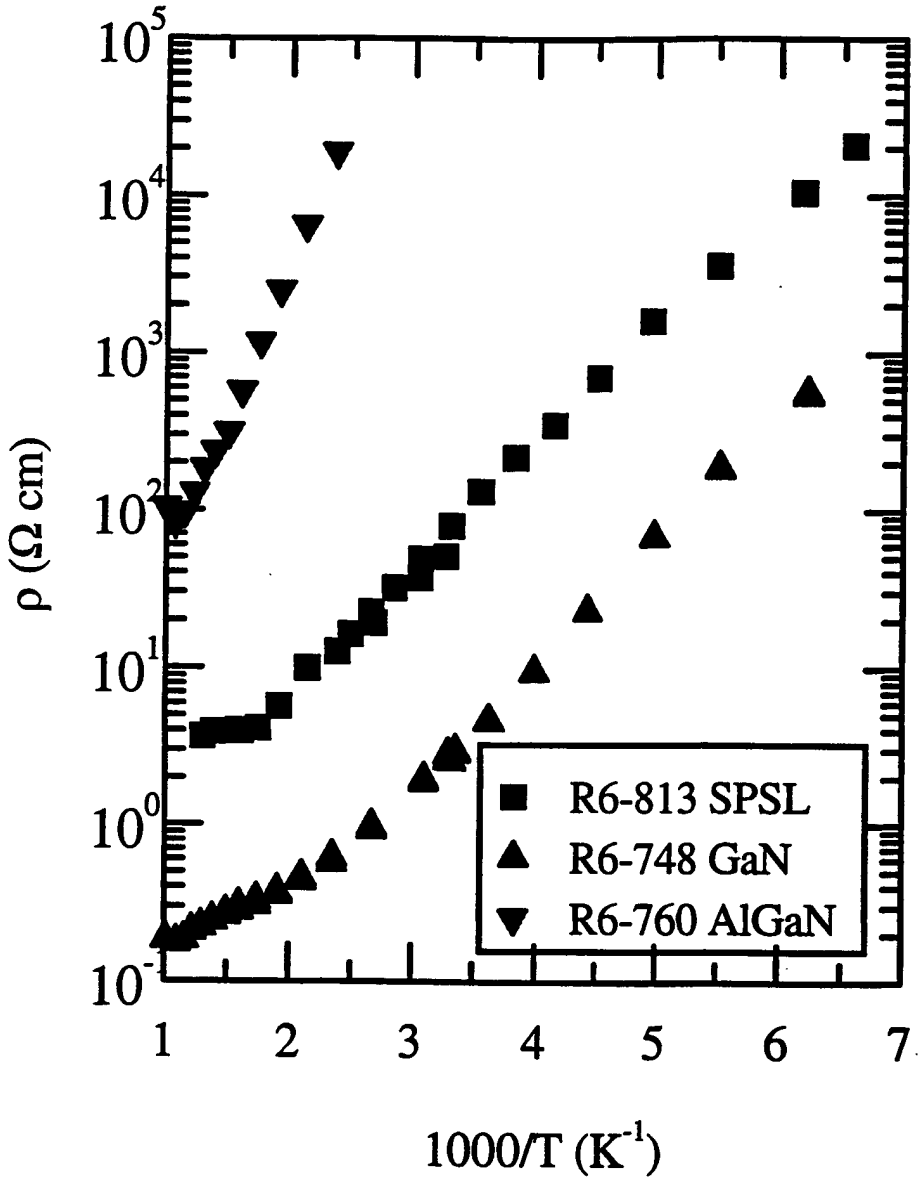

Figure 13. Temperature dependent resistivity of III-Nitride films.

The data from fits for several samples is summarized in Figure 14, which plots the acceptor ionization energy as a function of the cutoff wavelength at which 50% of the light is transmitted. These initial data points show that it is possible to lower the acceptor ionization energy for a given cutoff wavelength by using this doping technique. The increased ionization energy for the higher aluminum containing SPSL's could be due to a larger number of compensating donors changing the position where the Fermi level is pinned.

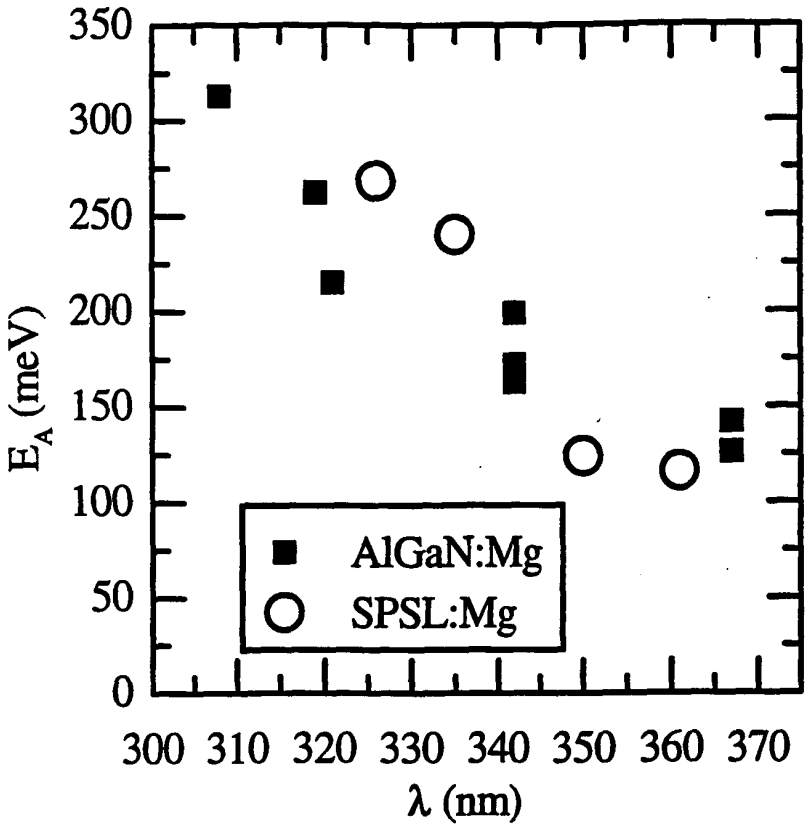

Figure 14. Acceptor ionization energies as a function of optical absorption edge (50% transmission) of bulk-like AlGaN:Mg compared with Mg doped GaN/AlGaN short-period superlattices.

4. CONCLUSIONS

Silicon doping of $Al_xGa_{1-x}N$ using dilute silane was studied. Low donor ionization energies were measured up to x=0.5. However, a film grown with x=0.7 had a much higher activation energy of 0.68 eV.

Short-period superlattices consisting of alternating layers of GaN:Mg and AlGaN:Mg were grown by low-pressure organometallic vapor phase epitaxy. The electrical properties of these superlattices were measured as a function of temperature and compared to conventional AlGaN:Mg layers. It is shown that the optical absorption edge can be shifted to shorter wavelengths while lowering the acceptor ionization energy by using short-period superlattice structures instead of bulk-like AlGaN:Mg. Since the hole effective mass is much larger than the electron effective mass, and the conduction band offset is larger than that of the valence band, most of the wavelength shift in the p-type SPSL will due to the energy shift in the conduction band. This should be beneficial for most optoelectronic devices based on this material. These initial results are very promising, and should encourage more detailed experimental and theoretical work, including application to devices.

ACKNOWLEDGMENTS

The authors wish to acknowledge the assistance of R. Perrin, G. Landis, and S. Davidson. The work at Northwestern University was supported in part by ONR/BMDO Grant N00014-93-1-0235 and DARPA/ONR Grant N00014-96-1-0714.

REFERENCES

1. M. Razeghi and A. Rogalski, "Semiconductor ultraviolet detectors," *J. Appl. Phys.* **79**, pp. 7433-7473, 1996.
2. O. Aktas, Z. F. Fan, S. N. Mohammed, A. E. Botchkarev, and H. Morkoç, "High temperature characteristics of AlGaN/GaN modulation doped field-effect transistors," *Appl. Phys. Lett.* **69**, pp. 3872-3874, 1996.
3. S. Nakamura, M. Seno, S. Nagahama, N. Iwasa, T. Yamada, T. Matsushita, Y. Sugimoto, and H. Kiyoku, "Room-temperature continuous-wave operation of InGaN multi-quantum-well structure laser diodes," *Appl. Phys. Lett.* **69**, pp. 4056-4058, 1996.
4. X. Zhang, P. Kung, A. Saxler, D. Walker, T. C. Wang, and M. Razeghi, "Growth of Al Ga N:Ge on sapphire and silicon substrates," *Appl. Phys. Lett.* **67**, pp. 1745-1747, 1995.
5 J. D. Guo, M. S. Feng, and F. M. Pan, Jpn. J. Appl. Phys. **34**, 5510 (1995).
6. A. Saxler, P. Kung, X. Zhang, D. Walker, J. Solomon, M. Ahoujja, W. C. Mitchel, H. R. Vydyanath, and M. Razeghi, "GaN doped with sulfur," *Materials Science Forum* **258-263**, pp. 1161-1166, 1997.
7. A. Saxler, D. Walker, P. Kung, X. Zhang, M. Razeghi, J. Solomon, W. C. Mitchel, and H. R. Vydyanath, "Comparison of trimethylgallium and triethylgallium for the growth of GaN," *Appl. Phys. Lett.* **71**, pp. 3272-3274, 1997.
8. A. Saxler, P. Kung, C. J. Sun, E. Bigan, and M. Razeghi, "High quality aluminum nitride epitaxial layers grown on sapphire substrates," *Appl. Phys. Lett.* **64**, pp. 339-341, 1994.
9. P. Kung, A. Saxler, X. Zhang, D. Walker, T. C. Wang, I. Ferguson, and M. Razeghi, "High quality AlN and GaN epilayers grown on (00•1) sapphire, (100), and (111) silicon substrates," *Appl. Phys. Lett.* **66**, pp. 2958-2960, 1995.
10. P. Kung, A. Saxler, X. Zhang, D. Walker, R. Lavado, and M. Razeghi, "Metalorganic chemical vapor deposition of monocrystalline GaN thin films on β-$LiGaO_2$ substrates," *Appl. Phys. Lett.* **69**, pp. 2116-2118, 1996.
11. X. Zhang, P. Kung, D. Walker, A. Saxler, and M. Razeghi, "Growth of GaN without yellow luminescence," *Mater. Res. Soc. Symp. Proc.* **395**, pp. 625-629, 1996.
12. A. Saxler, M. A. Capano, W. C. Mitchel, P. Kung, X. Zhang, D. Walker, and M. Razeghi, "High resolution X-ray diffraction of GaN grown on sapphire substrates," *Mater. Res. Soc. Symp. Proc.* **449**, pp. 477-482, 1997.
13. D. Walker, A. Saxler, P. Kung, X. Zhang, M. Hamilton, J. Diaz, and M. Razeghi, "Visible blind GaN p-i-n photodiodes," *Appl. Phys. Lett.* **72**, pp. 3303-3305, 1998.
14. D. Walker, X. Zhang, A. Saxler, P. Kung, J. Xu, and M. Razeghi, "$Al_xGa_{1-x}N$ ($0 \le x \le 1$) ultraviolet photodetectors grown on sapphire by metal-organic chemical-vapor deposition," *Appl. Phys. Lett.* **70**, pp. 949-951, 1997.
15 C. Stampfl and C. Van de Walle, "Doping of $Al_xGa_{1-x}N$," *Appl. Phys. Lett.* **72**, pp. 459-461, 1998.
16. M. Stutzmann, O. Ambacher, A. Cros, M. S. Brandt, H. Angerer, R. Dimitrov, N. Reinacher, T. Metzger, R. Höpler, D, Brunner, F. Freudenberg, R. Handschuh, and Ch. Deger, "Properties and applications of MBE grown AlGaN," *Mater. Science and Engineering* **B50**, pp. 212-218, 1997.
17. A. Saxler, *Exploration of LP-MOCVD Grown III-Nitrides on Various Substrates*, pp. 154-163, Northwestern University, Evanston, Illinois, 1998.
18. T. Tanaka, A. Watanabe, H. Amano, Y. Kobayashi, I. Akasaki, S. Yamazaki, and M. Koike, "*p*-type conduction in Mg-doped GaN and $Al_{0.08}Ga_{0.92}N$ grown by metalorganic vapor phase epitaxy," *Appl. Phys. Lett.* **65**, pp. 593-594, 1994.
19. I. Akasaki and H. Amano, "Crystal growth and conductivity control of group III nitride semiconductors and their application to short wavelength light emitters," *Jpn. J. Appl. Phys.* **36**, pp. 5393-5408, 1997.
20. S. Nakamura, "InGaN multiquantum-well-structure laser diodes with GaN-AlGaN modulation-doped strained-layer superlattices," *IEEE J. Selected Topics Quantum Electron.* **4**, pp. 483-489, 1998.
21. G. Bastard, *Wave Mechanics Applied to Semiconductor Heterostructures*, p. 21, Halsted Press, New York, 1988.